sponding to the two families described earlier. They do not agree with either the shock strength model estimation or the turbulent diffusion model as shown by Figs. 2 and 4. A possible explanation for this discrepancy is that Hall had measured the velocity of the source radiating into the outer flow by the mixing layer, which is not the large eddy convection velocity. The measurements made at IMST by Barre[22] confirm that Uc is different from the sound sources' velocity Us.

In conclusion, a new method, based on a shock strength parameter, was used to calculate the convective velocity of large-scale structures in a specific flow configuration corresponding to an assumption of convected shock waves linked to the eddies. From all of the results presented in this note, it appears that this assumption seems to adequately describe a large number of flows where the confinment ratio δ/D is of the order of 0.1. It has been shown that this model cannot describe nonconfined flows, which seem to behave in a more isentropic way.

Acknowledgment

The author would like to acknowledge many helpful conversations with J. P. Dussauge.

References

[1]Dimotakis, P. E., "Two-Dimensional Shear-Layer Entrainment," *AIAA Journal*, Vol. 24, No. 11, 1986, pp. 1791–1796.

[2]Brown, G. L., and Roshko, A., "On Density Effects and Large Structures in Turbulent Mixing Layers," *Journal of Fluid Mechanics*, Vol. 64, Pt. 4, 1974, pp. 775–781.

[3]Bogdanoff, D.W., "Compressibility Effects in Turbulent Shear Layers," *AIAA Journal*, Vol. 21, No. 6, 1983, pp. 926, 927.

[4]Papamoschou, D., "Experimental Investigation of Heterogeneous Compressible Shear Layers," Ph.D. Thesis, California Inst. of Technology, Pasadena, CA, 1986.

[5]Dimotakis, P. E., "Turbulent Free Shear Layer Mixing and Combustion," *High-Speed Flight Propulsion Systems*, edited by S.N.B. Murthy and E. T. Curran, Vol. 137, Progress in Astronautics and Aeronautics, AIAA, Washington, DC, 1991, pp. 265–340.

[6]Papamoschou, D., "Structure of the Compressible Turbulent Shear Layer," AIAA Paper 89-0126, Jan. 1989.

[7]Dimotakis, P. E., "On the Convection Velocity of Turbulent Structures in Supersonic Shear Layers," AIAA Paper 91-1724, Jan. 1991.

[8]Chinzei, N., Masuya, G., Komuro, T., Murakami, A., and Kudou, K., "Spreading of Two Stream Supersonic Turbulent Mixing Layer," *Physics of Fluids A*, Vol. 29, No. 5, 1986, pp. 1345–1347.

[9]Bradshaw, P., "The Effect of Initial Conditions on the Development of a Free Shear Layer," *Journal of Fluid Mechanics*, Vol. 26, Pt. 2, 1966, pp. 225–236.

[10]Liepmann, H., and Laufer, J., "Investigation of Free Turbulent Mixing," NACA TN 1257, 1947.

[11]Lau, J. C., Morris, P. J., and Fisher, M. J., "Measurements in Subsonic and Supersonic Free Jets Using a Laser Velocimeter," *Journal of Fluid Mechanics*, Vol. 93, Pt. 1, 1979, pp. 1–27.

[12]Wygnanski, I., and Fiedler, H., "The Two-Dimensional Mixing Region," *Journal of Fluid Mechanics*, Vol. 41, Pt. 2, 1970, pp. 327–362.

[13]Samimy, M., Petrie, H. L., and Addy, A. L., "A Study of Compressible Turbulent Reattaching Free Shear Layer," *AIAA Journal*, Vol. 24, No. 2, 1986, pp. 261–267.

[14]Elliott, G. S., and Samimy, M., "Compressibility Effects in Free Shear Layers," *Physics of Fluids A*, Vol. 2, No. 7, 1990, pp. 1231–1240.

[15]Ikawa, H., "Turbulent Mixing Layer Experiment in Supersonic Flow," Ph.D. Thesis, California Inst. of Technology, Pasadena, CA, 1973.

[16]Dutton, J. C., Burr, R. F., Goebel, S. G., and Messersmith, N. L., "Compressibility and Mixing in Turbulent Free Shear Layer," 12th Symposium on Turbulence, Paper A22, Rolla, MO, Sept. 1990.

[17]Petrie, H. L., Samimy, M., and Addy, A. L., "Compressible Separated Flows," *AIAA Journal*, Vol. 24, No. 12, 1986, pp. 1971–1978.

[18]Wagner, R. D., "Mean Flow and Turbulence Measurements in a Mach 5 Free Shear Layer," NASA TN D7366, 1973.

[19]Hall, J. L., "An Experimental Investigation of Structure, Mixing and Combustion in Compressible Turbulent Shear Layers," Ph.D. Thesis, California Inst. of Technology, 1991.

[20]Barre, S., Dupont, P., and Dussauge, J. P., "Convection Velocity of Large Scale Structures in a Supersonic Mixing Layer," *IUTAM Symposium on Eddy Structure Identification in Free Turbulent Shear Flows*, Centre d'Etude Aérodynamique et Thermique, (Poitiers, France), Oct. 1992, pp. XI.7.1–XI.7.5.

[21]Si-Ameur, M., Gathmann, R., Chollet, J. P., and Mathey, F., "Turbulence dans les Écoulements Supersoniques Libres ou Confinés, Couches de Mélange et Jets," *Colloque sur les Écoulements Hypersoniques* Laboratoire d'Aérothermique de Medoun, (Medoun, France), Oct. 5–7 1992, pp. 213–220.

[22]Barre, S., "Action de la Compressibilité sur la Structure des Couches de Mélange Turbulentes Supersoniques," Thèse de doctorat de l'Ecole Nationale Supériere de l'Aéronautique et de l'Espace, Toulouse, France, defended on Jan. 6, 1993.

[23]Samimy, M., Reeder, M. F., and Elliott, G. S., "Compressibility Effects on Large Structures in Free Shear Flows," *Physics of Fluids A*, Vol. 4, No. 6, 1992, pp. 1251–1258.

Quasiglobal Reaction Model for Ethylene Combustion

D. J. Singh*
Analytical Services and Materials Inc., Hampton, Virginia 23666
and
Casimir J. Jachimowski†
NASA Langley Research Center, Hampton, Virginia 23681

Introduction

THE current interest in hypersonic flight has created a resurgence of interest in hypersonic airbreathing propulsion systems. In this flight regime, most of the work has concentrated on hydrogen-fueled supersonic combustion ramjet engines. For a Mach number range of 4–10, hydrocarbon fuels provide sufficient thrust and are also being considered. The high density of hydrocarbon fuels, as well as ease of handling, makes them very attractive for volume-constrained systems such as missiles and the hypersonic research vehicle (HRV).

The design of future hypersonic propulsion systems will depend very heavily on computational fluid dynamics (CFD) because of the difficulties associated with testing combustors in ground-based facilities at flight speeds. Therefore, it is essential to develop CFD codes capable of numerically simulating the hostile environment of a combustor. The numerical simulation of conservative equations, including a detailed kinetics system for a multidimensional system, is computationally prohibitive, if not impossible. Even with the availability of supercomputers, routine computations of combustor flowfields are not possible. Most of the computer codes that include detailed chemical kinetics are limited to one dimension. In order to help CFD design the engine, a real need exists for the development of reduced mechanisms. In this study, attention will be focused on ethylene (C_2H_4). Ethylene is chosen because it is used as a surrogate test fuel for hydrocarbon fuels. Also, because ethylene is usually an intermediate product in the combustion of heavy hydrocarbons, the developed model can also be used for assembling reaction mechanisms of heavy hydrocarbons such as propane, butane, n-heptane, etc. Westbrook and Dryer[1] developed a two-step reaction mechanism for ethylene. The assumption of CO, CO_2, and H_2O as the final products overpredicts the heat of reaction; hence, a higher flame temperature results. This model was developed primarily for laminar flame calculations and would not be adequate for combustor application.

The objective of this study is to develop a reduced mechanism for ethylene oxidation. We are interested in a model with a minimum number of species and reactions that still models the chemistry with reasonable accuracy for the expected combustor conditions. The model will be validated by comparing the results to those calculated with a detailed kinetic model that has been validated against the experimental data. The detailed ethylene mecha-

Received Nov. 21, 1992; revision received May 21, 1993; accepted for publication June 9, 1993. This paper is declared a work of the U.S. Government and is not subject to copyright protection in the United States.

*Research Scientist, 107 Research Drive. Member AIAA.

†Chief Combustion Chemist, Hypersonic Propulsion Branch, Fluid Mechanics Division. Member AIAA.

nism used in this study is the mechanism assembled by Jachimowski.[2]

Approach

In this study, a global chemical modeling approach is used. The major features of the chemical reaction, such as temperature, pressure, induction time, and final concentration of species, are examined. The generality of the model is sacrificed to reduce the number of species and reactions. The method used for obtaining the reduced mechanism is that proposed by Edelman and Fortune.[3] In this method, the oxidation of hydrocarbon fuel is described by a single global reaction of the form

$$\text{fuel} + O_2 \rightleftharpoons CO + H_2 \tag{1}$$

The remaining reactions in the mechanism describe in detail the oxidation of CO and H_2. Following this approach the oxidation of ethylene is described by a single global reaction

$$C_2H_4 + O_2 \rightleftharpoons 2CO + 2H_2 \tag{2}$$

This reaction is then followed by nine other reactions which describe the oxidation of CO and H_2. The rate of these reactions are given by the equation

$$R = AT^n \exp(E/RT) \tag{3}$$

The reduced reaction system and the constants A, n, and E are given in Table 1. The rate coefficient for reaction (1) was empirically determined to obtain a good agreement in the final temperature and temperature profile between the reduced and the detailed

Table 1 C_2H_4 - O_2 reaction system[a] (10 step)

No.	Reaction[b]	A	n	E
1	$C_2H_4 + O_2 \rightleftharpoons 2CO + 2H_2$	$1.80E+14$	0.0	35,500
2	$CO + O \rightleftharpoons CO_2 + M$	$5.30E+13$	0.0	−4540
3	$CO + OH \rightleftharpoons CO_2 + H$	$4.40E+06$	1.5	−740
4	$H_2 + O_2 \rightleftharpoons OH + OH$	$1.70E+13$	0.0	48,000
5	$H + O_2 \rightleftharpoons OH + O$	$2.60E+14$	0.0	16,800
6	$OH + H_2 \rightleftharpoons H_2O + H$	$2.20E+13$	0.0	5150
7	$O + H_2 \rightleftharpoons OH + H$	$1.80E+10$	1.0	8900
8	$OH + OH \rightleftharpoons H_2O + O$	$6.30E+13$	0.0	1090
9	$H + H \rightleftharpoons H_2 + M$	$6.40E+17$	−1.0	0
10	$H + OH \rightleftharpoons H_2O + M$	$2.20E+22$	−2.0	0

[a]Units are in seconds, moles, cubic centimeters, calories, and degrees Kelvin. [b]Third-body efficiencies for all thermolecular reactions are 2.5 for $M = H_2$, 16.0 for H_2O, and 1.0 for all other M.

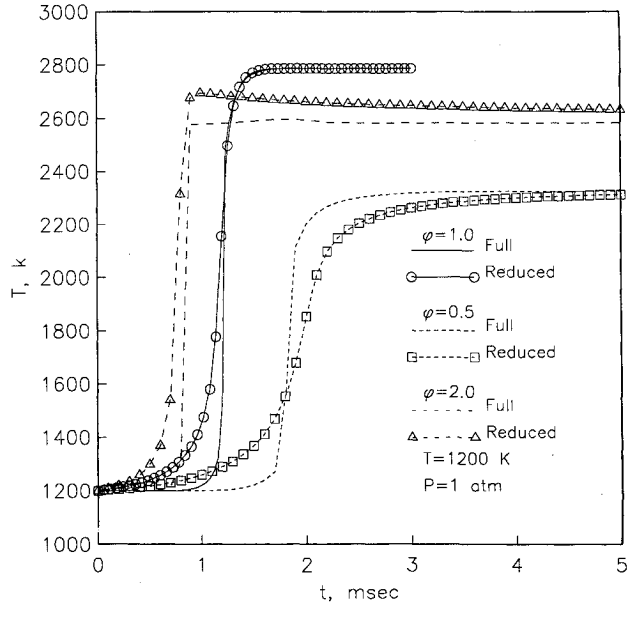

Fig. 1 Temperature profile for 1 atm of pressure at 1200 K.

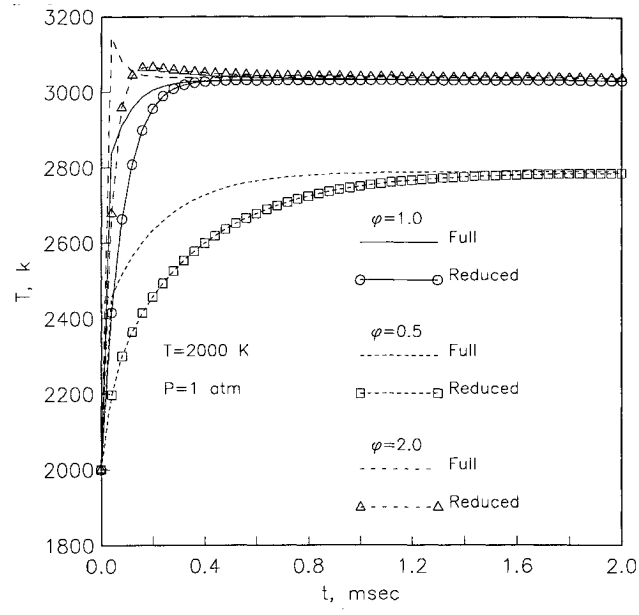

Fig. 2 Temperature profile for 1 atm of pressure at 2000 K.

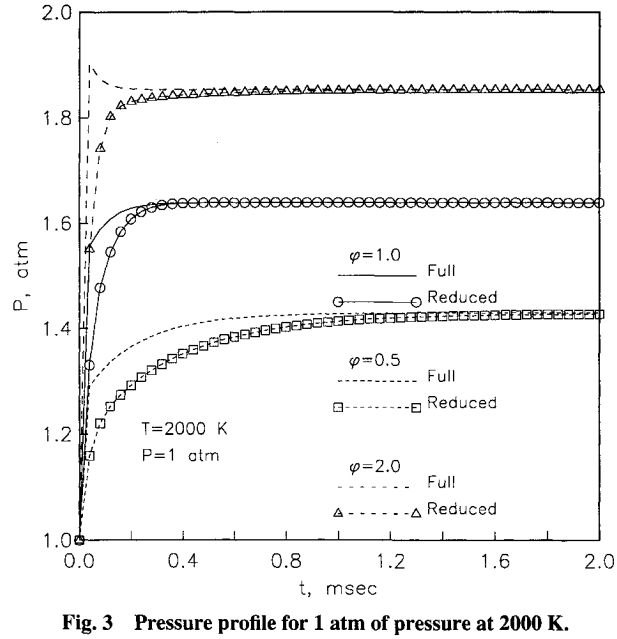

Fig. 3 Pressure profile for 1 atm of pressure at 2000 K.

mechanisms over the anticipated combustor conditions. The coefficients for the remaining reactions are the same as those in the detailed mechanism. The model was then tested over a range of pressure, temperature, and equivalence ratios to assess its validity. This procedure is similar to that used to determine the constants for detailed mechanisms, except that the detailed model is used here as a reference rather than the experimental data.

A computer program described in Ref. 4 was used to compute a one-dimensional, steady-state, constant-density flowfield with both detailed and reduced mechanisms. At constant density, the volume of the system remains constant, and if no heat flows in or out of the system, the direct effect of the chemical reaction should be evident in the temperature profiles.

Results and Discussion

A wide range of initial conditions were computed: pressure (0.5–2.0 atm), temperature (1200–2000 K), and ϕ (0.5–2.0). Figure 1 shows the time variation of temperature with an initial temperature of 1200 K and 1-atm pressure for various values of ϕ, computed with the use of both detailed and reduced mechanisms. Time is

expressed in milliseconds. For ϕ = 1.0, both models predict an almost identical profile, except in the initial stages. The final temperature agrees very well. As expected, for other values of ϕ, the temperature drops. At ϕ = 0.5, the temperature profile differs in that the temperature rise begins earlier and takes longer to reach the final temperature. Here again, good agreement for the final temperature can be seen between the two models. As the value of ϕ is increased to 2.0, the reduced model overpredicts the temperature by about 4%. In general, the reduced model predicted shorter ignition delay as compared to the complete mechanism.

Figure 2 shows the comparison between the detailed and the reduced model for a temperature of 2000 K and 1-atm pressure. The temperature is underpredicted during the initial stage, but the final temperature agrees very well for all values of fuel/air ratio conditions. As a result of a higher initial temperature, the mixture attains the final temperature much earlier than the case shown in Fig. 1. The heat-release characteristics are reproduced very well by the reduced model.

The pressure profiles for an initial temperature of 2000 K and 1-atm pressure are shown in Fig. 3. For ϕ = 2.0, the pressure has an overshoot, but then asymptotes to the right value. For all cases, the pressure is slightly underpredicted in initial stages, but the overall agreement between the two models is very good for all values of ϕ.

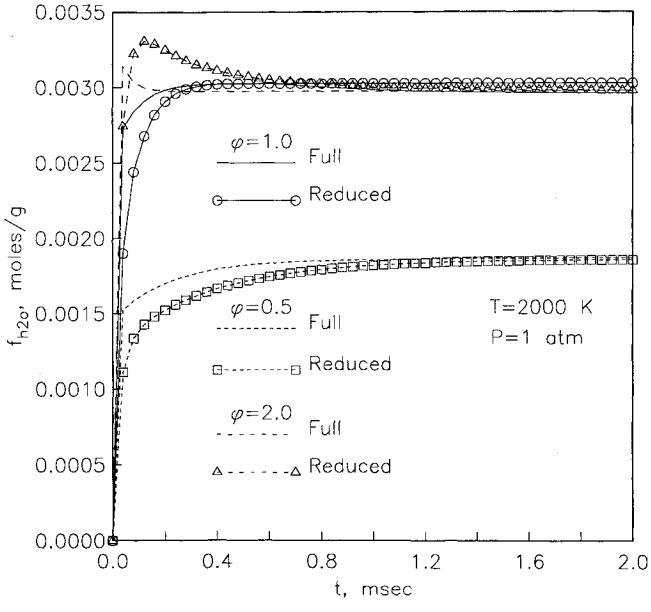

Fig. 4 Concentration of H_2O for 1 atm of pressure at 2000 K.

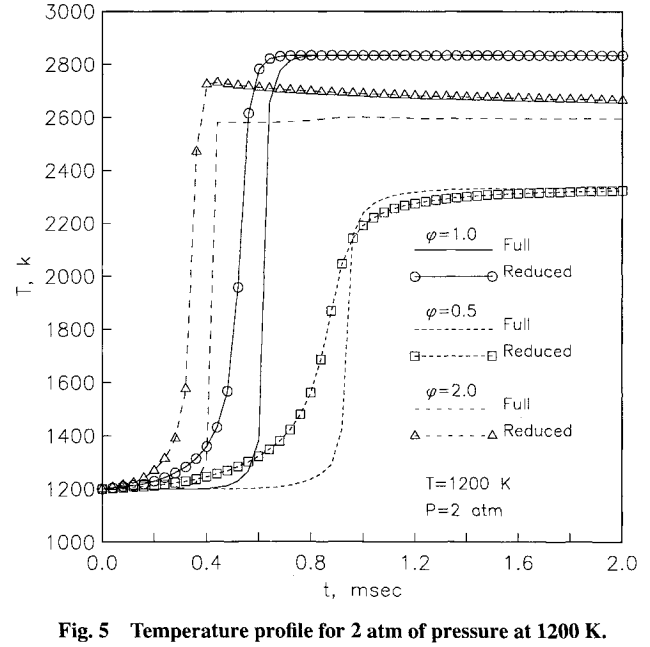

Fig. 5 Temperature profile for 2 atm of pressure at 1200 K.

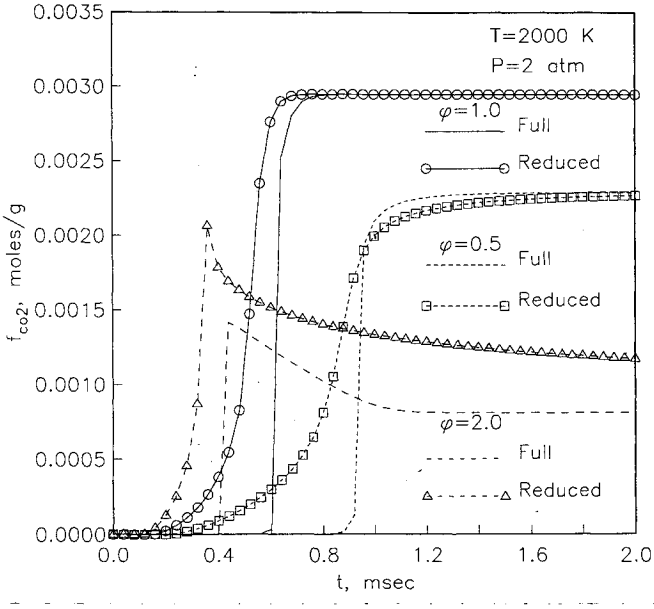

Fig. 6 Concentration of CO_2 for 2 atm of pressure at 1200 K.

A comparison between the two models in terms of H_2O concentration can be seen in Fig. 4 for a temperature of 2000 K and 1 atm of pressure. The concentration of H_2O agrees very well between the two models for various values of ϕ. Initially, the reduced model has an overshoot in H_2O concentration for ϕ = 2.0, but then settles down to the correct concentration. For ϕ = 1.0 and 0.5, the concentrations are slightly underpredicted initially; however, correct final values are predicted.

All of the results discussed so far were computed for initial pressure of 1 atm. To determine the validity of the model at higher pressure, calculations were performed at a pressure of 2 atm and a temperature of 1200 K. The temperature and CO_2 profiles are shown in Figs. 5 and 6, respectively. The results in Fig. 5 are similar to those in Fig. 1, except that the fuel burns faster at the higher pressure. Figure 6 shows the variation of CO_2 concentration. For ϕ = 1.0 and 0.5, the concentration asymptotes to that the correct value, but for ϕ = 2.0, the reduced model overpredicts the concentration. Also, the reduced model shows that the formation of CO_2 begins earlier than it does in the detailed model.

Conclusion

A quasiglobal model for finite-rate combustion of ethylene is assembled and compared with the detailed reaction mechanism. The results obtained by using the reduced mechanism compare very well with the detailed model under a wide range of physical conditions. The reduced model consists of 9 species and 10 reactions, a significant reduction from the detailed model which has 25 species and 77 reactions. The present model can be easily incorporated into the existing CFD codes without significantly increasing the computational costs. The study shows that the quasiglobal modeling approach can be used to develop finite-rate combustion models when the intermediate chemical kinetic reactions are either not known or are not of interest.

References

[1]Westbrook, C. K., and Dryer, F. L., "Simplified Reaction Mechanisms for the Oxidation of Hydrocarbon Fuels in Flames," *Combustion Science and Technology*, Vol. 27, No. 1–2, 1981, pp. 31–43.

[2]Jachimowski, C. J., "An Experimental and Analytical Study of Acetylene and Ethylene Oxidation Behind Shock Waves," *Combustion and Flame*, Vol. 29, No. 1, 1977, pp. 55–66.

[3]Edelman, R. B., and Fortune, O. F., "A Quasi-Global Chemical Kinetic Model for the Finite Rate Combustion of Hydrocarbon Fuels with Application to Turbulent Burning and Mixing in Hypersonic Engines and Nozzles,"

AIAA 7th Aerospace Sciences Meeting, AIAA Paper 69-96, New York, Jan. 1969.

[4]McLain, A. G., and Rao, C. S. R., "A Hybrid Computer Program for Rapidly Solving Flowing or Static Chemical Kinetics Involving Many Chemical Species," NASA TM X-3403, July 1976.

Numerical Study of Unsteady Supersonic Compression Ramp Flows

S. O. Park,* Y. M. Chung,† and H. J. Sung‡
Korea Advanced Institute of Science and Technology, Taejon 305-701, Republic of Korea

Introduction

TWO-DIMENSIONAL, steady, inviscid, supersonic flows past a compression ramp are very well known. However, unsteady flows past a moving compression ramp with time varying wedge angle have received scant attention and are thus little understood. Degani and Steger[1] touched upon the compression-ramp flow where the ramp moved from 15 to 20 deg at a constant angular velocity. In that work, the main interest was the comparison between the thin-layer and the Navier-Stokes computation. We intend in this work to investigate inviscid supersonic flow past a moving compression ramp by numerically solving the Euler equations. The flow configuration is schematically shown in Fig. 1a. Despite its simple geometry, such a flow can hardly be tackled by analytical means since linearization is not allowed. The wedge angle varies linearly with time from 0 deg up to a given angle. When the wedge angle reaches the final value, the ramp motion ceases. The flow configuration may be considered as a fundamental problem for transient flow of a thrust vectoring nozzle or a maneuvering high-speed wing. Important parameters for the present flow are the free stream Mach number M_∞, the angular velocity of the wedge Ω, and the final wedge angle Θ_f. A pertinent dimensionless parameter from these variables is the reduced angular velocity $\bar{\Omega}$ defined by the relation $\bar{\Omega} = \Omega L/M_\infty a_\infty$, where L is a reference length. The flow is anticipated to change significantly with $\bar{\Omega}$ and thus several typical values of were considered in this work.

Numerics

The equations to be solved are the two-dimensional Euler equations in conservation form. When the governing equation is integrated over a fixed control volume A with boundary surface C, we obtain

$$\iint_A \left(\frac{\partial w}{\partial t}\right) dA + \oint_C (f\,dy - f\,dx) \tag{1}$$

where $w = (\rho, \rho u, \rho v, \rho e)^T$, and f and g are appropriate flux vectors corresponding to w (Ref. 2).

When the control volume is moving with velocity, where $\zeta = (\xi, \eta)^T$, the material derivative of volume integral can be written as follows via the Reynolds' transport theorem:

$$\frac{d}{dt}\iint_{A(t)} w\,dA = \iint_A \left(\frac{\partial w}{\partial t}\right) dA + \int_C w(\zeta \cdot \boldsymbol{n})\,ds \tag{2}$$

Received Dec. 31, 1992; presented as Paper 93-0883 at the AIAA 31st Aerospace Sciences Meeting, Reno, NV, Jan. 11–14, 1993; revision received June 8, 1993; accepted for publication June 12, 1993.

*Professor, Department of Aerospace Engineering, 373-1 Kusong-Dong, Yusung-Ku. Member AIAA.

†Research Assistant, Department of Mechanical Engineering, 373-1 Kusong-Dong, Yusung-Ku.

‡Associate Professor, Department of Mechanical Engineering, 373-1 Kusong-Dong, Yusung-Ku.

Using Eq. (2), Eq . (1) can be written for a moving control volume as[3]

$$\frac{d}{dt}(Aw) + qw = 0 \tag{3}$$

where A is the area of a grid cell and

$$qw = \oint_C [(f - w\xi)\,dy - (g - w\eta)\,dx] + \text{artificial dissipation terms} \tag{4}$$

For the artificial dissipation terms, we adopted Jameson's second- and fourth-order expressions[4,5] Equation (3) was integrated using the fourth-order Runge-Kutta time-stepping scheme.[4] For inflow and upper far boundaries, free-stream conditions were specified. Outflow boundary values were specified using second-order extrapolation from the interior node values. Transient solutions were obtained by time-marching Eq. (3) with uniform flow at time $t = 0$. The grid system over the surface of the wedge moves in the x and y directions with the speed of the moving wedge. Preliminary computations were carried out for the case of $\bar{\Omega} = 0.1$ for the wedge with $M_\infty = 2$ and $\Theta_f = 20$ deg on 40×40, 60×60, and 80×80 mesh systems. All of the three mesh systems performed to yield solutions accurate within 0.5% compared with the analytic solutions for the steady flow. However, for the unsteady flow, the solutions with the 40×40 mesh system were of poor quality when compared with the solutions with the 60×60 and 80×80 mesh systems. The solutions with the 80×80 mesh system were essentially the same as those with the 60×60 mesh system. Thus, we chose the 60×60 mesh system for the present work. The time increment Δt (for the unsteady calculations) was chosen to make the Courant-Friedrichs-Lewy (CFL) number be 0.1 when $\bar{\Omega} = 1.0$ and 0.2 when $\bar{\Omega} = 0.1$ or smaller. The solutions of the exploratory computations with the CFL number of 0.5 exhibited spurious wiggles across the shock wave during the motion of the ramp. Since the present computation required time accurate solutions, we conservatively chose CFL numbers to be small as stated earlier.

Results and Discussion

The transient solutions were obtained for the cases of four different values of angular velocity $\bar{\Omega}$ with $M_\infty = 2$, and $\Theta_f = 20$ deg.

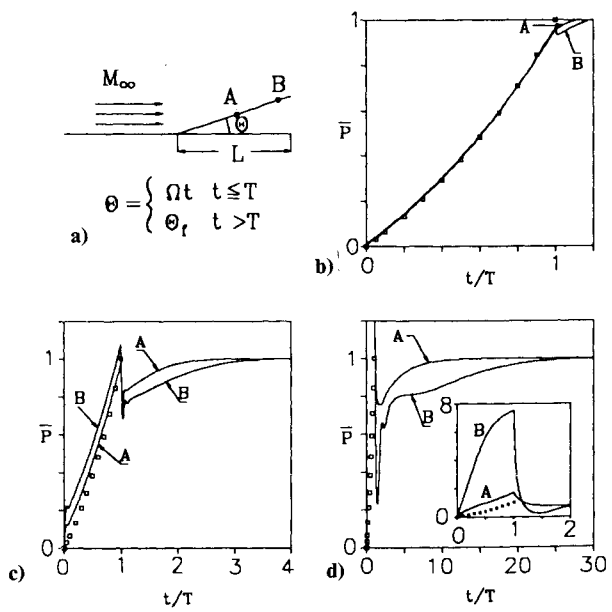

Fig. 1 Flow configuration and surface pressure variation $\{\bar{p} = (p - p_\infty)/[p(t = \infty)] - p_\infty\}$: a) schematic, b) $\bar{\Omega} = 0.01$, c) $\bar{\Omega} = 0.1$, and d) $\bar{\Omega} = 1.0$.